Uncertainties on atomic data. A case study: N IV

G. Del Zanna [1]★ L. Fernández-Menchero [2] and N. R. Badnell [3]

[1]*DAMTP, Centre for Mathematical Sciences, University of Cambridge, Wilberforce Road, Cambridge CB3 0WA, UK*
[2]*CTAMOP, Queen's University of Belfast, Belfast BT7 1NN, UK*
[3]*Department of Physics, University of Strathclyde, Glasgow G4 0NG, UK*

ABSTRACT

We consider three recent large-scale calculations for the radiative and electron-impact excitation data of N IV, carried out with different methods and codes. The scattering calculations employed the relativistic Dirac R-matrix (DARC) method, the intermediate coupling frame transformation (ICFT) R-matrix method, and the B-spline R-matrix (BSR) method. These are all large-scale scattering calculations with well-tested and sophisticated codes, which use the same set of target states. One concern raised in previous literature is related to the increasingly large discrepancies in the effective collision strengths between the three sets of calculations for increasingly weak and/or high-lying transitions. We have built three model ions and calculated the intensities of all the main spectral lines in this ion. We have found that, despite such large differences, excellent agreement (to within ± 20 per cent) exists between all the spectroscopically relevant line intensities. This provides confidence in the reliability of the calculations for plasma diagnostics. We have used the differences in the radiative and excitation rates amongst the three sets of calculations to obtain a measure of the uncertainty in each rate. Using a Monte Carlo approach, we have shown how these uncertainties affect the main theoretical ratios that are used to measure electron densities and temperatures.

Key words: atomic data – techniques: spectroscopic.

1 INTRODUCTION

With the advances in computational power, an increasing number of large-scale atomic calculations for ions of astrophysical importance have become available in the past few years. Within several communities, there is now awareness of the importance of the accuracy of atomic calculations for astrophysical applications. The IAEA has organized a workshop on uncertainties of atomic data, and some guidance is provided in e.g. Chung et al. (2016). Within the solar community, Guennou et al. (2013) used some general estimates of available rates, to assess uncertainties on the temperature distribution of the solar plasma, obtained by combining spectroscopic observations with atomic data. The resulting uncertainties were large. A much better approach is to assess in some way the uncertainty in each single rate, by e.g. comparing theory with experiment or results of different calculations. One of us (GDZ) developed such an approach, and used comparisons of two calculations to assess uncertainties associated with line ratios used to measure electron densities from Fe XIII (Yu et al. 2018). A general overview of some of the uncertainties in atomic data is presented in Del Zanna & Mason (2018).

For most astrophysical plasmas that are collisional (i.e. not photoionized), the main rates affecting the spectral lines of an ion are those of spontaneous decay (A-values), and those of collisional excitation by electron impact. In this paper, we focus on the latter, considering that they are normally the most complex ones to calculate accurately. The main quantity is the effective collision strength Υ of a transition, which is the rate obtained from the adimensional cross-section (the collision strength) assuming a Maxwellian distribution of the electrons.

Historically, large discrepancies in the effective collision strengths calculated with different approximations and codes were present. However, with the advances in computational power, results have generally converged for low-lying transitions. However, in the recent literature, several cases have now appeared where differences of up to one or two orders of magnitude for weak and/or high-lying transitions have been found. This clearly raises concerns on the reliability of any of such calculations, and their effects on diagnostic applications.

Generally, the effective collision strengths to the lower levels of an ion agree to within ± 20 per cent, although in a few cases they can differ significantly. One such example are the calculations for the coronal Fe XI ion, where the values calculated by Del Zanna, Storey & Mason (2010) were generally in good agreement (within ± 20 per cent) with those calculated by Aggarwal & Keenan (2003), with the exception of a few amongst the strongest ones, where large

differences were present. They occurred for levels that have a strong spin–orbit interaction, so the calculations are very sensitive to the atomic structure.

We are concerned here with those cases where the overall results are significantly different. There are several examples in the literature, some of which have been recently reviewed by Aggarwal (2017). For example, Aggarwal & Keenan (2014) used the Dirac Atomic *R*-matrix Code (DARC) of P. H. Norrington and I. P. Grant to calculate effective collision strengths for the important coronal Fe XIV. They found large discrepancies with the results obtained by Liang et al. (2010) with the Intermediate Coupling Frame Transformation (ICFT) *R*-matrix method (Griffin, Badnell & Pindzola 1998). The Aggarwal & Keenan (2014) calculations adopted much smaller configuration-interaction (CI) and close-coupling (CC) expansions than the previous study, so significant differences are to be expected. Indeed, Del Zanna et al. (2015a) carried out a new ICFT calculation with the same CC/CI expansions as that one adopted by Aggarwal & Keenan (2014) and found excellent agreement between the DARC and ICFT results. The main differences between the smaller DARC and the larger ICFT calculation was the CC expansion used.

A similar case concerns Al X. Aggarwal & Keenan (2015) carried out a DARC 98-levels calculation on this ion, showing significant differences with the results obtained by Fernández-Menchero, Del Zanna & Badnell (2014) with a much larger (238-level) ICFT calculation. As in the Fe XIV case, Fernández-Menchero, Del Zanna & Badnell (2015) carried out ICFT and Breit–Pauli *R*-matrix calculations with the same target (98-levels) adopted by Aggarwal & Keenan (2015), and the results were shown to agree closely. Various comparisons were also provided, showing how both the choices of CC and CI expansions can significantly affect the collision strengths.

On a side note, we stress that it has been shown in the literature that when the atomic structure of an ion is similar, and the same CI/CC expansions are adopted, results of the DARC and ICFT are very similar (see e.g. Liang, Whiteford & Badnell 2009; Liang & Badnell 2010; Badnell & Ballance 2014). Clearly, many other issues affect the final results, such as the energy resolution and the threshold positions, but are often of less importance, as we have discussed e.g. in the Badnell et al. (2016) review.

There are also reported differences in collision strengths obtained with other codes. For example, Aggarwal & Keenan (2017) carried out a DARC *R*-matrix calculation on Mg V on 86 target states and found large, order of magnitude differences for weak and/or high-lying transitions with two previous results. One was an earlier (and smaller) ICFT *R*-matrix calculation carried out by Hudson et al. (2009). The other one, by Tayal & Sossah (2015), was on the same 86 target states but used a completely different approach, the B-spline *R*-matrix (BSR) method (see e.g. Zatsarinny 2006; Zatsarinny & Bartschat 2013, for details).

In a recent study, Wang et al. (2017) carried out two sets of BSR calculations, one with the same 86 target states as in Tayal & Sossah (2015), but with a more accurate representation of the target structure; the other one was a much larger calculation with 316 states. Close agreement with the previous BSR calculations was found when the smaller calculation was considered. Significant increases in the collision strengths of the weaker transitions was however found when the much larger calculation was considered. We note that such results are common and are mostly due to extra resonances, and coupling in general, which can increase the cross-sections for weak transitions. Differences with the DARC results were found.

For the present study we have chosen to consider the Be-like N IV, as effective collision strengths obtained with the DARC, ICFT, and BSR *R*-matrix codes are now available. They were obtained with the same set of target states, hence are directly comparable. Aggarwal, Keenan & Lawson (2016) carried out a DARC scattering calculation for N IV, showing order of magnitude discrepancies for many weak and/or high-lying transitions with the values calculated previously by Fernández-Menchero et al. (2014) with the ICFT *R*-matrix codes [hereafter ICFT results]. The DARC calculations adopted the same set of configurations for the CI/CC expansions as those used by Fernández-Menchero et al. (2014). Therefore, in principle one would expect good agreement, at least for those transitions where slight differences in the atomic structure (which are always present) are not significant.

To shed light into this issue, Fernández-Menchero, Zatsarinny & Bartschat (2017) recently carried out a large-scale calculation with the BSR codes. Good agreement between all calculations was found for the strong transitions within the low-lying states. Significant increasing differences with both the ICFT and DARC results were found for the increasingly weaker and/or higher transitions. The differences are attributable to the inherent lack of convergence in the target CI expansion and/or the collisional CC expansion in all three calculations, which increasingly affects the weaker and/or higher lying transitions. The convergence study by Fernández-Menchero et al. (2015) illustrates this point.

In this paper, we focus on two important aspects: (1) we show that the large differences have negligible effects for astrophysical modelling; (2) we use the differences as a measure of the uncertainty in the rates, and provide a measure of the uncertainty in derived quantities such as electron densities.

It is well known that a few of the strongest N IV lines are useful diagnostics for astrophysical plasma (e.g. nebulae and the solar corona), see e.g. Dufton, Doyle & Kingston (1979). Some have also been used in laboratory plasma (tokamaks).

2 MODELLING SPECTRAL LINE INTENSITIES

2.1 Atomic data

Aggarwal et al. (2016) carried out two sets of atomic structure calculations using the GRASP (General-purpose Relativistic Atomic Structure Package) code, originally developed by Grant et al. (1980) and then revised by P. H. Norrington. We consider here only the larger one, which the authors labelled as GRASP2. This considered configuration interaction (CI) producing the same set of 238 fine-structure levels adopted by Fernández-Menchero et al. (2014). They included a relatively complete set of configurations up to principal quantum number $n = 5$, plus 72 levels arising from $n = 6, 7$ configurations, which was added by Fernández-Menchero et al. (2014) to improve the structure for the lower levels.

Fernández-Menchero et al. (2014), on the other hand, used the AUTOSTRUCTURE (AS) program (Badnell 2011) and radial wavefunctions calculated in a scaled Thomas–Fermi–Dirac–Amaldi statistical model potential. As shown by Aggarwal et al. (2016), some differences in the energies of the two calculations are present, although not apparently large enough to expect large differences in the results of the scattering calculations.

For the scattering calculations, Aggarwal et al. (2016) used the relativistic DARC program. For the comparisons shown here we only consider the results of their 'DARC2' calculation, which included in the CC expansion the same set of 238 levels of the CI.
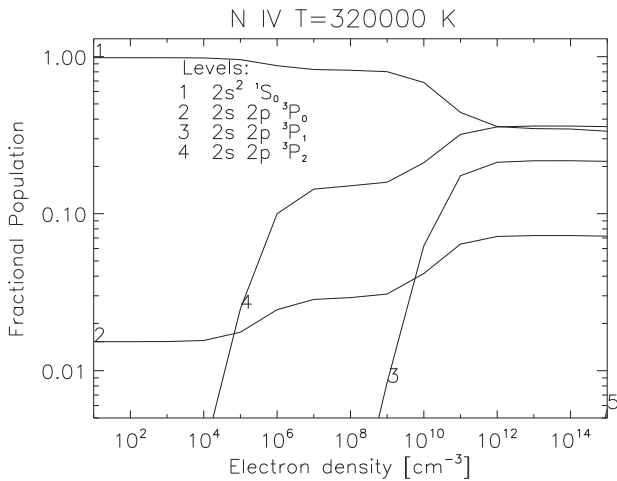
Figure 1. Relative populations of the levels of N IV.

Fernández-Menchero et al. (2014) instead used a set of codes and methods some of which originated from the Iron Project, and are described in e.g. Hummer et al. (1993) and Berrington, Eissner & Norrington (1995). The *R*-matrix inner region calculation was in *LS*-coupling and included both mass–velocity and Darwin relativistic energy corrections. For the outer region, the ICFT method was applied to the *LS*-coupled *K*-matrices calculated with the STGF code (Badnell and Seaton, unpublished). Collision strengths were 'topped-up' to infinite partial waves following Burgess (1974) and Badnell & Griffin (2001). Finally, the collision strengths were extended to high energies by interpolation using the appropriate high-energy limits in the Burgess & Tully (1992) scaled domain. The high-energy limits were calculated with AUTOSTRUCTURE following Burgess, Chidichimo & Tully (1997) and Chidichimo, Badnell & Tully (2003).

As we mentioned, Fernández-Menchero et al. (2017) carried out a large-scale calculation with the BSR codes. They included all the valence configurations {2s, 2p, 3s, 3p, 3d} *nl* of N^{3+}. The outer valence–electron *nl* wavefunction was expanded in a basis set of 134 B-splines of order 8. The BSR calculation was limited to the total angular momenta $J = 0-6$, obtaining a total of 1400 levels, including bound and continuum. Of these 1400 levels calculated, 238 were included in the later CC expansion. They used the same outer region STGF code, but now in *jK*-coupling.

We used the collision strengths and *A*-values published by Fernández-Menchero et al. (2017) to calculate the level population for this ion at the temperature of maximum abundance in ionization equilibrium. We used the codes available within the CHIANTI package (Dere et al. 1997; Del Zanna et al. 2015b). Fig. 1 shows that for any astrophysical density, and for any plasma laboratory density below 10^{15} cm^{-3}, the levels that drive the population of all the levels in the ion are the ground state ($2s^2\ ^1S_0$) and the three metastable levels, from the 2s 2p ^3P. This is an important issue: the intensities of the spectral lines are directly proportional to the populations of the upper levels, which in turn are driven solely by the collision rates from these four lower levels. All the rates from the other levels are irrelevant for the modelling.

We therefore looked at the gf values (weighted oscillator strengths) of all the transitions from these four levels, as calculated by Aggarwal et al. (2016) with GRASP and Fernández-Menchero et al. (2014) with AS. They are shown in Fig. 2 (top). With very few notable exceptions, there is excellent agreement, to within
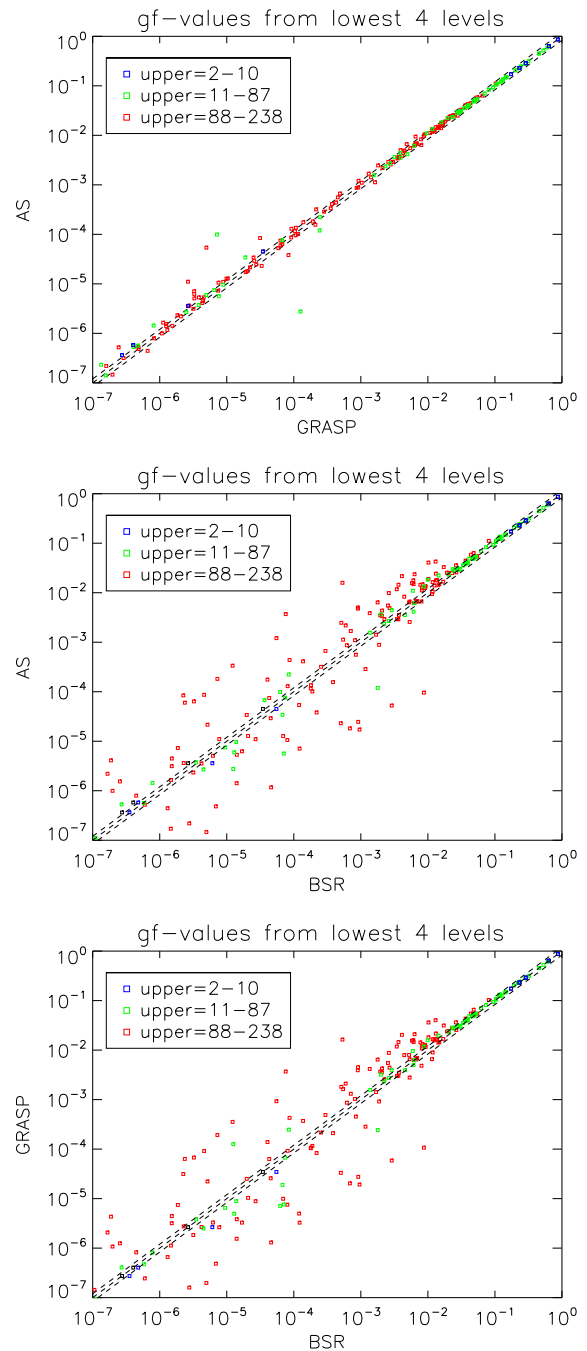
Figure 2. Comparisons of gf-values as calculated with the GRASP, AS, and BSR codes for all transitions from the metastable levels. Dashed lines show ±20 per cent.

±20 per cent, for all the transitions, especially the strong ones. On the other hand, significant differences (over ±20 per cent) with the BSR calculated values are present for the weaker transitions, as shown in the two lower plots of Fig. 2.

Such differences become even more evident when all the transitions are considered, as shown in Fig. 2 of Fernández-Menchero et al. (2017). These differences result directly from the different method used in the atomic structure calculation. The BSR calculations adopted a multi-configuration Hartree–Fock (MCHF) expansion that included the continuum in the form of pseudo-orbitals, and where the radial functions for the outer valence electron

were expanded in a B-spline basis. This generated different non-orthogonal sets of one-electron orbitals for each target state and the continuum, and therefore led to a more extended CI expansion, compared to the GRASP and AS results. In particular, CI included configuration mixing with the additional [3s, 3p, 3d]nl bound states, as well as the interaction with the continuum. One would expect that the use of a more complete basis set in the BSR calculations would provide a better atomic structure. Indeed, as shown in Fernández-Menchero et al. (2017), the resultant level energies are the ones closest to the observed values (as available in NIST or CHIANTI).

The comparison of the Υ as calculated with the DARC, ICFT, and BSR codes, for the same set of transitions, at temperatures close to ion peak abundance, are shown in Fig. 3. Excellent agreement (to within ± 20 per cent) between the DARC and ICFT is found for all transitions, with a few cases belonging to the higher levels (2p 4l and most of the n = 6, 7, above level No. 87) that deviate by only about 30 per cent. As in the case of the gf values, larger differences are found with the BSR values. This is expected as the high-temeprature limits of the effective collisions strengths are directly related to the gf values.

The larger deviations occur for the transitions to higher levels, which are mostly forbidden. Such variations are quite typical for weak forbidden lines, which are very sensitive to a number of issues, such as cancellation effects, the positioning of the resonances, etc. Much larger variations are present if one considers all transitions from all levels, as shown by Aggarwal et al. (2016) and Fernández-Menchero et al. (2017). However, as we pointed out, they would not have any effect for the modelling.

The question is whether the 30–40 per cent variations in the forbidden lines have any significant effect on the level population for this ion. To assess this, we have build three ion models and solved the level population.

### 2.2 Level population and line intensities

Within an atomic database such as CHIANTI (Del Zanna et al. 2015b), one typically merges the Υ from a calculations with ad hoc, normally more accurate, radiative data (*A*-values) obtained by a completely different calculation. Among the three calculations we consider, as we have mentioned the BSR one has the best atomic structure so we have adopted the BSR *A*-values, and built three model ions, with the BSR, ICFT, and DARC effective collision strengths. We had to switch the indexing of several levels in the ICFT and DARC calculations, for a meaningful comparison.

All the excitations between all 238 levels were retained, although as we pointed out, only those from the lowest four levels are needed to model plasma emission below 10^{15} cm^{-3}. We have used the CHIANTI codes to calculate the line emissivities, finding the level populations by including the proton rates as available in CHIANTI v.8.

Since for diagnostic application one is interested in relative ratios, we have considered the spectral line emissivities, normalized to the intensity of the strongest resonance line, the 2s^2 ^{1}S$_0$–2s 2p ^{1}P$_1$ at 765 Å.

Fig. 4 shows the ratios of the spectral line intensities as calculated with the ICFT, DARC, and BSR collision strengths. The intensities have been calculated at ion peak abundance (log T[K] = 5.15) and at an electron density of 10^{11} cm^{-3}, close to the value expected in a solar active region.

Despite the order of magnitude differences in some of the collision strengths, Fig. 4 clearly shows that there is an excellent agreement, to within ±20 per cent, for all the spectroscopically relevant lines that are within four orders of magnitude the brightest
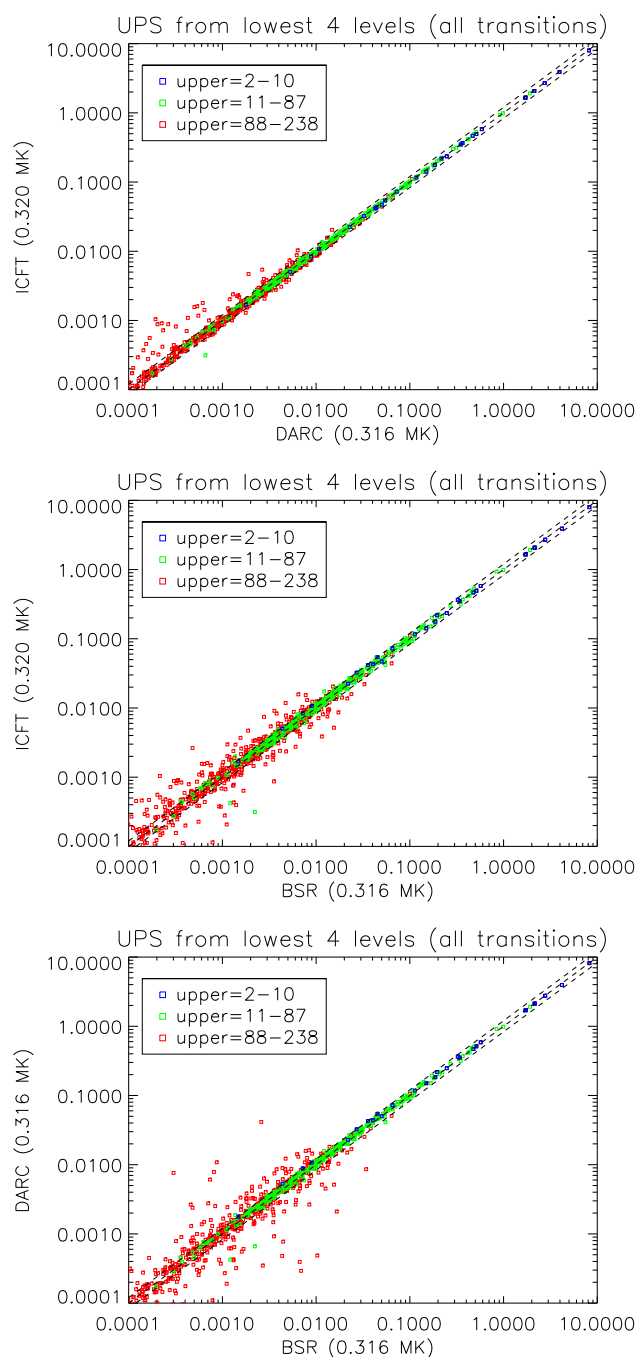

Figure 3. Comparisons of effective collision strengths Υ (UPS) near ion peak abundance as calculated with the DARC, ICFT, and BSR codes, for all transitions from the metastable levels.

line. Larger differences, but still within about 50 per cent, are present for all the other extremely weak and spectroscopically unobservable lines. Interestingly, agreement improves when the models based on the ICFT and DARC collision strengths are compared directly. In some respects, the ICFT and DARC calculations are based on atomic structure calculations that are different but of similar accuracy.

## 3 ESTIMATING UNCERTAINTIES ON THE MAIN DIAGNOSTIC RATIOS

As reviewed in Del Zanna & Mason (2018), lines of Be-like ions have been extensively used in astrophysics to measure electron
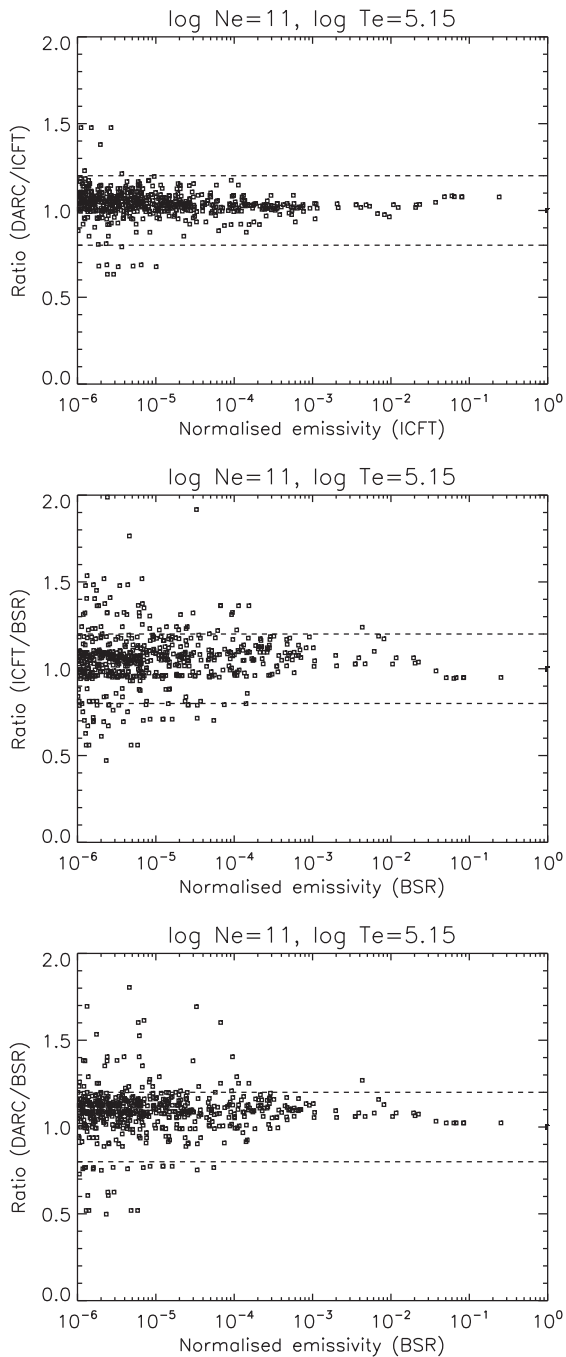
Figure 4. Ratios of all the spectral line intensities, calculated with the three model ions, based on the ICFT, DARC, and BSR Υ values, as a function of their normalized intensities (i.e. relative to the strength of the resonance line). Dashed lines indicate ± 20 per cent.

densities and temperatures. It is therefore useful to assess the impact of the uncertainties in the atomic rates on the main ratios.

Similarly to the Fe XIII study (Yu et al. 2018), we have taken a 'Monte Carlo' approach, i.e. we have calculated the level populations and line emissivities 100 times by randomly varying each A-value and collisional rate within some bounds, using the BSR values as a reference. To define the bounds for each rate, we have compared the three calculated values and taken the maximum relative deviation from the BSR values. We have limited the variation to a minimum of 2 per cent (as some variations are smaller
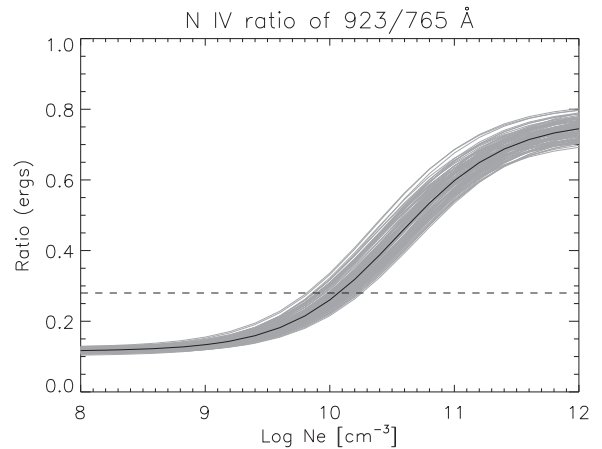
Figure 5. Main density diagnostic for N IV at log $T[K] = 5$. The dashed line indicates the quiet Sun observed value reported by Dufton et al. (1979).
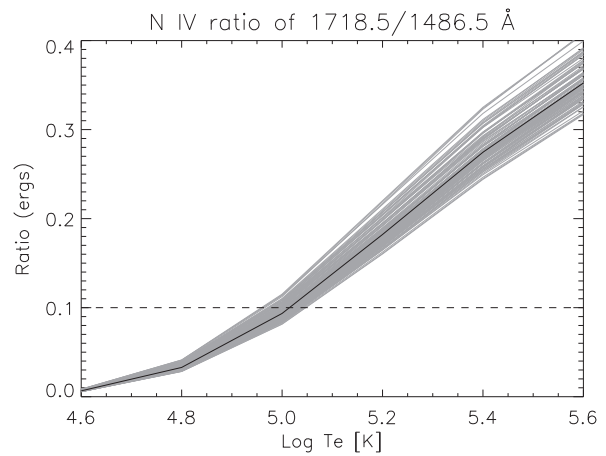
Figure 6. Main electron temperature diagnostic for N IV, calculated at an electron density of 10^{10} cm^{-3}. The dashed line indicates the quiet Sun observed value reported by Dufton et al. (1979).

than this) and a maximum of 80 per cent, neglecting the few order of magnitude variations that, as we have shown, have little effect on the line intensities. Unlike Yu et al. (2018), where a normal distribution was adopted (with standard deviation equal to the bound), we have adopted a strict random distribution within the bounds.

The main ratio to measure electron densities is that of the multiplet of transitions from the $2p^2$ ^3P to the $2s2p$ ^3P to the resonance line, the $2s^2$ $^1S_0$–$2s$ $2p$ $^1P_1$ at 765 Å. The multiplet of lines falls around 923 Å and is blended with other transitions. Dufton et al. (1979) reported a deblended ratio of 0.28 for the quiet Sun, and found an electron density of 1.5×10^{10} cm^{-3}, assuming a temperature of formation of log $T[K] = 5.1$ and using the atomic data available at the time. Fig. 5 shows the theoretical ratio obtained from the BSR data (black line) and the 99 random realizations (grey lines) for log $T[K] = 5$. The dashed line indicates the quiet Sun observed value reported by Dufton et al. (1979). We can see that we obtain a similar value, about 1.2×10^{10} cm^{-3}, with an uncertainty of about 0.2 in dex.

The main ratio to measure electron temperatures is the 2s 2p $^1P_1$–$2p^2$ $^1D_2$ (1718.5 Å) versus the $2s^2$ $^1S_0$–2s 2p $^3P_1$ (1486.5 Å). Fig. 6 shows the the theoretical ratio obtained from the BSR data (black line) and the 99 random realizations (grey lines), calculated for an electron density of 10^{10} cm^{-3}. The dashed line indicates the quiet

Sun observed value reported by Dufton et al. (1979). We can see that we obtain a temperature of log $T[K] = 5$, the same value estimated by Dufton et al. (1979). The uncertainty is about 0.05 in dex.

Clearly, a proper evaluation of the uncertainties should also include the uncertainties in the observed values. Also, it should include a model of how the densities and temperatures might vary along the line of sight, as the emissivities of the lines we have considered are dependent on both the electron densities and temperatures, to some degree. Such model would depend critically on the source region observed. As the observations of the two ratios reported by Dufton et al. (1979) were not simultaneous and were obtained in different conditions by different instruments, it is not possible to further explore this aspect in this example.

4 CONCLUSIONS

We have considered three independent calculations of the effective collision strengths for N IV which, for many transitions, show large order of magnitude discrepancies for many weak transitions and/or those involving high-lying levels.

At first glance, such differences are of concern for astrophysical applications, although we should point out that thay are inherent in *R*-matrix CC methods based-on truncated CI and/or CC expansions. We view such discrepancies as an excellent way to provide a measure on the uncertainty in calculating rates for weak transitions and to high-lying levels.

Despite the differences, we have shown that in the case of N IV excellent agreement (to within a relative 20 per cent) is found among the line intensities obtained from the three independent calculations considered here, for the spectroscopically and astrophysically important emission lines. Agreement in the line intensities obtained with the ICFT and the DARC effective collision strengths is even better, to within a relative 10 per cent.

The present modelling clearly shows that the few forbidden transitions where the BSR, DARC, and ICFT collision strengths differ significantly are not really relevant for any astrophysical application where densities are below 10^{15} cm^{-3}. If low densities such in astrophysical nebulae are considered, the discrepancies are even smaller, because the level populations are driven solely by the excitation rates from the ground state, as this is the only populated level (cf. Fig. 1).

We expect similar results for the other ions along the Be-like sequence. The metastable levels become populated at increasingly higher densities along the sequence (with increasing atomic number). Therefore, we would expect for the higher Z elements better agreement in the line intensities calculated from the different codes for say solar densities (10^8–10^{12} cm^{-3}).

We have used the differences obtained by the three sets of calculations as a measure of the uncertainty in each of the radiative and collisional rates. With simple Monte Carlo simulations, we have shown how such uncertainties affect the main diagnostic applications for this ion, to measure electron densities and temperatures. We suggest that such an approach should be adopted when estimating uncertainties on the theoretical ratios.

REFERENCES

Aggarwal K., 2017, Atoms, 5, 37
Aggarwal K. M., Keenan F. P., 2003, A&A, 399, 799
Aggarwal K. M., Keenan F. P., 2014, MNRAS, 445, 2015
Aggarwal K. M., Keenan F. P., 2015, MNRAS, 447, 3849
Aggarwal K. M., Keenan F. P., 2017, Can. J. Phys., 95, 9
Aggarwal K. M., Keenan F. P., Lawson K. D., 2016, MNRAS, 461, 3997
Badnell N. R., 2011, Comput. Phys. Commun., 182, 1528
Badnell N. R., Ballance C. P., 2014, ApJ, 785, 99
Badnell N. R., Griffin D. C., 2001, J. Phys. B: At. Mol. Phys., 34, 681
Badnell N. R., Del Zanna G., Fernández-Menchero L., Giunta A. S., Liang G. Y., Mason H. E., Storey P. J., 2016, J. Phys. B: At. Mol. Phys., 49, 094001
Berrington K. A., Eissner W. B., Norrington P. H., 1995, Comput. Phys. Commun., 92, 290
Burgess A., 1974, J. Phys. B: At. Mol. Phys., 7, L364
Burgess A., Tully J. A., 1992, A&A, 254, 436
Burgess A., Chidichimo M. C., Tully J. A., 1997, J. Phys. B: At. Mol. Phys., 30, 33
Chidichimo M. C., Badnell N. R., Tully J. A., 2003, A&A, 401, 1177
Chung H.-K., Braams B. J., Bartschat K., Császár A. G., Drake G. W. F., Kirchner T., Kokoouline V., Tennyson J., 2016, J. Phys. D: Appl. Phys., 49, 363002
Del Zanna G., Mason H. E., 2018, Living Rev. Solar Phys., 5, 15
Del Zanna G., Storey P. J., Mason H. E., 2010, A&A, 514, A40
Del Zanna G., Badnell N. R., Fernández-Menchero L., Liang G. Y., Mason H. E., Storey P. J., 2015a, MNRAS, 454, 2909
Del Zanna G., Dere K. P., Young P. R., Landi E., Mason H. E., 2015b, A&A, 582, A56
Dere K. P., Landi E., Mason H. E., Monsignori Fossi B. C., Young P. R., 1997, A&AS, 125, 149
Dufton P. L., Doyle J. G., Kingston A. E., 1979, A&A, 78, 318
Fernández-Menchero L., Del Zanna G., Badnell N. R., 2014, A&A, 566, A104
Fernández-Menchero L., Del Zanna G., Badnell N. R., 2015, MNRAS, 450, 4174
Fernández-Menchero L., Zatsarinny O., Bartschat K., 2017, J. Phys. B: At. Mol. Phys., 50, 065203
Grant I. P., McKenzie B. J., Norrington P. H., Mayers D. F., Pyper N. C., 1980, Comput. Phys. Commun., 21, 207
Griffin D. C., Badnell N. R., Pindzola M. S., 1998, J. Phys. B: At. Mol. Phys., 31, 3713
Guennou C., Auchère F., Klimchuk J. A., Bocchialini K., Parenti S., 2013, ApJ, 774, 31
Hudson C. E., Ramsbottom C. A., Norrington P. H., Scott M. P., 2009, A&A, 494, 729
Hummer D. G., Berrington K. A., Eissner W., Pradhan A. K., Saraph H. E., Tully J. A., 1993, A&A, 279, 298
Liang G. Y., Badnell N. R., 2010, A&A, 518, A64
Liang G. Y., Whiteford A. D., Badnell N. R., 2009, A&A, 500, 1263
Liang G. Y., Badnell N. R., Crespo López-Urrutia J. R., Baumann T. M., Del Zanna G., Storey P. J., Tawara H., Ullrich J., 2010, ApJS, 190, 322
Tayal S. S., Sossah A. M., 2015, A&A, 574, A87
Wang K., Fernández-Menchero L., Zatsarinny O., Bartschat K., 2017, Phys. Rev. A, 95, 042709
Yu X. et al., 2018, ApJ, 866, 146
Zatsarinny O., 2006, Comput. Phys. Commun., 174, 273
Zatsarinny O., Bartschat K., 2013, J. Phys. B: At. Mol. Phys., 46, 112001

This paper has been typeset from a TEX/LATEX file prepared by the author.